ACS Catalysis

Letter

pubs.acs.org/acscatalysis

Cascade Reactions for the Continuous and Selective Production of Isobutene from Bioderived Acetic Acid Over Zinc-Zirconia Catalysts

Anthony J. Crisci,‡ Herui Dou,‡ Teerawit Prasomsri, and Yuriy Román-Leshkov*

Department of Chemical Engineering, Massachusetts Institute of Technology, 77 Massachusetts Avenue, Cambridge, Massachusetts 02139, United States

Supporting Information

ABSTRACT: Bio-oil (obtained from biomass fast pyrolysis) contains a high concentration of acetic acid, which causes problems related to its storage and handling. Acetic acid was upgraded directly to isobutene over a $Zn_xZr_yO_z$ binary metal oxide. The reaction proceeds via a three-step cascade involving ketonization, aldol condensation, and C−C hydrolytic bond cleavage reactions, which was corroborated by isotopic labeling studies. Separately, ZnO and ZrO_2 are incapable of producing isobutene from either acetic acid or acetone. In contrast, under optimal conditions, a $Zn_2Zr_8O_z$ catalyst generates a ca. 50% isobutene yield, which corresponds to 75% of the theoretical maximum. Spectroscopic investigations revealed that a balanced concentration of acid and base sites is required to maximize isobutene yields.

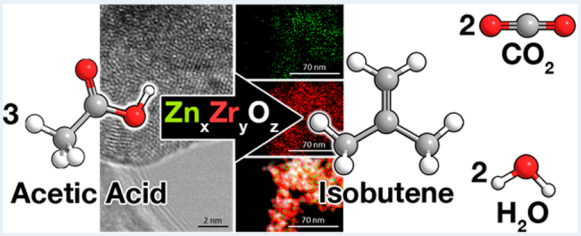

KEYWORDS: *pyrolysis oil, ketonization, aldol condensation, binary metal oxides, ZnO, ZrO_2, acetic acid, isobutene*

Upgrading bio-oil obtained from biomass fast pyrolysis into chemicals that are fungible with traditional petrochemicals is a major techno-economic challenge.[1] Crude bio-oil is a complex mixture of oxygenates containing a high concentration of carboxylic acids.[2] Acetic acid, the most abundant organic acid, may compose up to 12 wt % of the bio-oil.[3,4] Consequently, untreated bio-oil is corrosive to metals (e.g., engines, storage vessels) and promotes unwanted polymerization reactions, severely hindering its utility.[5,6]

Ketonization, wherein two organic acid molecules undergo C−C coupling to form a ketone, water, and carbon dioxide, is often cited as an effective method to neutralize and upgrade organic acids.[7−12] When it is coupled with hydrodeoxygenation, higher-value unsaturated hydrocarbons are produced from carboxylic acids. For instance, ketonization of acetic acid generates acetone, and hydrogenolysis of the resulting carbonyl functional group produces propene.[13] However, this tandem process may not be economical for upgrading low-value, small oxygenates because it requires hydrogen gas.[14] Alternatively, it has been shown that acetone can be converted to isobutene over zeolites such as H-ZSM-5, H-Y, and H-Beta.[15−18] Using these materials at temperatures above 333 K, acetone is first condensed to form diacetone alcohol. Next, the alcohol is converted into isobutene by dehydration to mesityl oxide and subsequent cleavage. Isobutene is a valuable product used to manufacture fuel additives (e.g., ETBE, MTBE, tri-isobutene), materials such as butyl rubber, and various other valuable chemicals.[19−21]

Recently, Sun et al. reported on the ability of ZrO_2 and ZnO catalysts to selectively convert ethanol to ethylene and acetone, respectively. Interestingly, their bifunctional $Zn_1Zr_{10}O_z$ catalyst (synthesized via hard templating) possessed different reactivity than the parent oxides.[22] Reacting ethanol over $Zn_1Zr_{10}O_z$ (the optimal Zn/Zr ratio) selectively produced isobutene. The mechanism was hypothesized to occur through sequential aldol and cracking reactions. However, mechanistic details for the proposed steps involving the condensation of ethanol to acetone and the cracking of the presumed intermediate, mesityl oxide, into isobutene was not provided. Therefore, developing a process that can couple ketonization, condensation, and cracking of bio-oil derived acetic acid into isobutene over a single catalyst is highly desirable. Furthermore, investigating the involved reaction pathways is equally important toward understanding and ultimately predicting the capabilities of these catalysts.

Herein, we report the selective and direct production of isobutene from acetic acid with an inexpensive binary oxide, $Zn_xZr_yO_z$, through a three-stage cascade reaction system in a continuous flow reactor, Scheme 1. We provide, by way of ^{13}C isotopic labeling and spectroscopic studies (vide infra), insight into the reaction pathways involved in this conversion. First, two acetic acid molecules ketonize to form acetone, water, and CO_2 over the oxide surface through an acetoacetic acid intermediate.[23] Next, acetone undergoes self-condensation through an aldol pathway to generate the enone, mesityl oxide, as the main product. Mesitylene and isophorone were also formed as minor byproducts. To complete the cycle, the enone undergoes a C−C bond cleavage step producing isobutene and acetic acid. Under optimal conditions, a $Zn_2Zr_8O_z$ catalyst generated a maximum isobutene yield of

Received: July 16, 2014
Revised: September 15, 2014
Published: October 21, 2014

   dx.doi.org/10.1021/cs501018k | ACS Catal. 2014, 4, 4196−4200

Scheme 1. Proposed Catalytic Cycle of Acetic Acid Conversion to Isobutene[a]

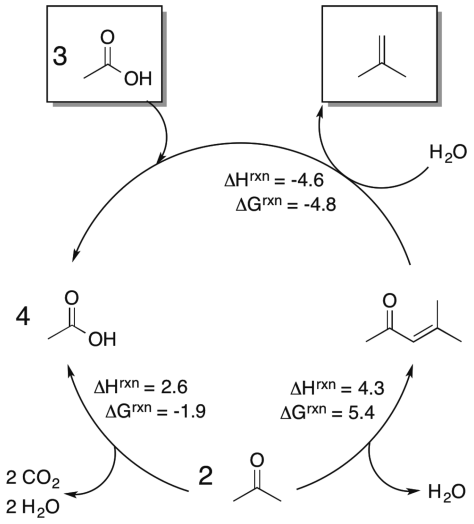

[a]All energies are reported in kcal·mol^{-1}.

50%, which corresponds to 75% of the theoretical yield (67% on a carbon basis). These results represent a drastic increase in isobutene production when compared to the hitherto highest yield of 15% obtained with ZSM-5 for this reaction.[17]

The presence of Zn in $Zn_xZr_yO_z$ enables the consecutive reactions required to transform acetic acid to isobutene. In general, heteroatom dopants alter adsorbate-binding strength and generate unsaturated metal cations/oxygen vacancies that affect the acid–base and redox chemistry of the oxide.[24] Additionally, the acid–base properties of metal oxides can be modulated by their degree of crystallinity, particle size, concentration of heteroatom dopants, and thermal treatment.[25,26] Zirconia is already an efficient ketonization catalyst yet selectivity enhancements are achieved by the addition of heteroatoms.[27] For example, the additions of Ce or Mg are thought to increase both the basicity and reducibility of the catalyst leading to higher ketone selectivities.[28−30] There are many mixed metal oxide combinations that can be obtained with Zn or Zr; however, there are few accounts for $Zn_xZr_yO_z$ solid solutions.[22,31−33]

A series of $Zn_xZr_yO_z$ solid solutions with various ratios of Zn to Zr (1:9, 2:8, 3:7 and 5:5) were synthesized via sol–gel method and characterized. Nitrogen adsorption studies revealed the overall surface area of the mixed oxide decreased when increasing the overall content of Zn. Specifically, for the samples with Zn/Zr ratios of 1:9 and 5:5, the Brunauer–Emmett–Teller (BET) surface areas were 166 and 63 $m^2 \cdot g^{-1}$, respectively. The $Zn_2Zr_8O_z$ solid solution and the physical-mixed ZnO/ZrO_2 (2:8; mole basis) possessed similar surface areas of 110 and 107 $m^2 \cdot g^{-1}$, respectively. At all Zn/Zr ratios, reflections corresponding to the tetragonal or monoclinic crystal phases of ZrO_2 were not observed by powder X-ray diffraction (PXRD) (see Figure 1). For Zn/Zr ratios higher than 3:7, weak diffractions associated with ZnO crystalline domains were visible. In contrast, $Zn_xZr_yO_z$ synthesized via hard templating yielded ZrO_2 crystal domains at all Zn/Zr ratios.[22] The lack of crystallinity in the sol–gel oxides suggests a more intimate relation between Zn and Zr than what is achieved by hard templating. As a representative sample, $Zn_2Zr_8O_z$ was imaged by transmission electron microscopy

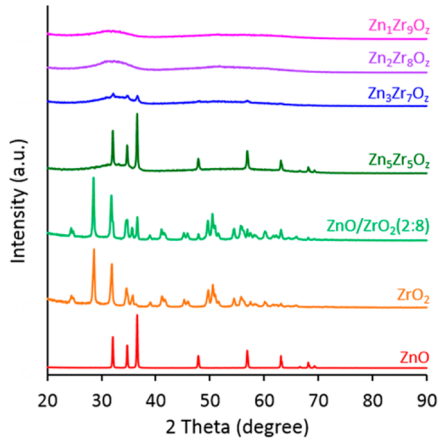

Figure 1. Powder X-ray diffraction patterns of various metal oxides.

(TEM) with energy-dispersive X-ray (EDX) spectroscopy (see Figure 2). No regular structural order was apparent and

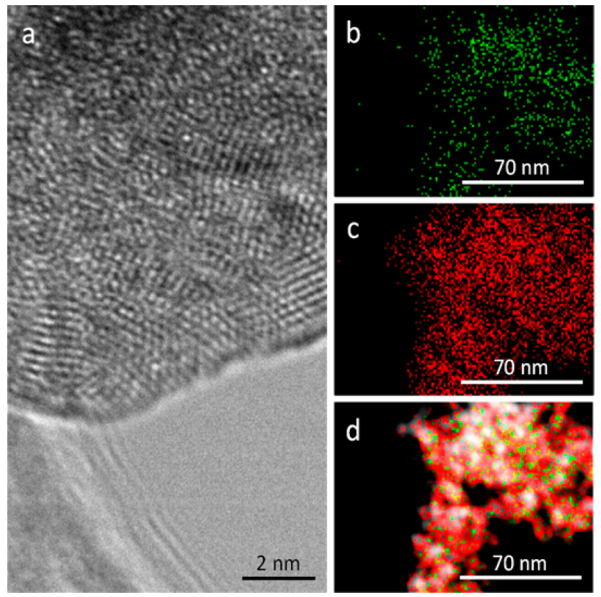

Figure 2. Images of $Zn_2Zr_8O_z$: (a) HR-TEM; (b) EDX elemental mapping– Zn channel; (c) EDX elemental mapping – Zr channel; (d) EDX elemental mapping – Zn/Zr composite.

elemental mapping showed a homogeneous distribution of Zn throughout the sample. Table S1 shows the acid–base properties of the various metal oxides assessed by temperature-programmed desorption (TPD). In general, the binary oxides (physically mixed and solid solutions) possessed significantly fewer acid sites and more basic sites relative to ZrO_2. Furthermore, the homogeneous distribution of Zn in $Zn_xZr_yO_z$ profoundly affects the acid–base properties of the constituent oxide. For example, despite possessing similar surface areas, $Zn_2Zr_8O_z$, ZnO/ZrO_2 (2:8) and ZrO_2 chemisorb 66, 246, and 355 $\mu mol \cdot g^{-1}$ of ammonia, and 241, 66, and 89 $\mu mol \cdot g^{-1}$ of carbon dioxide, respectively.

To successfully catalyze the reactions involved in the proposed cascade (Scheme 1), both acid and base sites are required. Although ZnO (wurtzite) and ZrO_2 (tetragonal) are both amphoteric oxides,[25] ZnO is generally considered to be a weak base, and ZrO_2 is an acid. Independently, neither oxide is active for the conversion of acetic acid to isobutene (yield

dx.doi.org/10.1021/cs501018k | ACS Catal. 2014, 4, 4196−4200

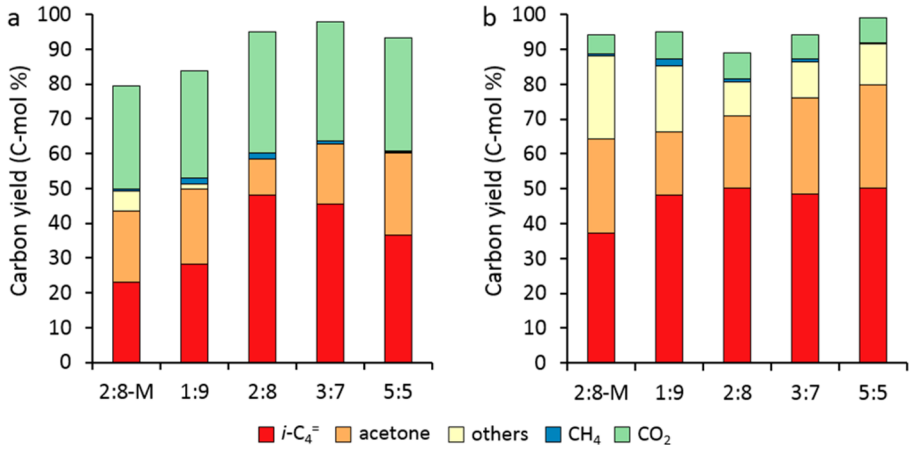

Figure 3. Conversion of (a) acetic acid and (b) acetone on $Zn_xZr_yO_z$ with varying Zn/Zr w/w ratios. Reaction conditions: T = 723 K, P = 1 atm, catalyst mass = 4 g, WHSV = 6.25 $g_{acetic\ acid}$ $(g_{cat.}\cdot h)^{-1}$ or 4.7 $g_{acetone}$ $(g_{cat.}\cdot h)^{-1}$, time = 4 h. Catalyst 2:8-M refers to a physical mixture of ZnO and ZrO_2; "others" refers to the sum of hexenones and mesitylene.

<3%). Although both catalysts are active and highly selective for the ketonization reaction of acetic acid to acetone, they are drastically less active and selective for the aldol condensation step of acetone to mesityl oxide. Specifically, at 723 K and a WHSV of 25 g_{feed} $(g_{cat.}\cdot h)^{-1}$, ZnO and ZrO_2 generate acetone yields from acetic acid of 55 and 70% at 67 and 95% conversion, respectively. Note that the theoretical carbon yield for acetone obtained through the ketonization reaction is 75%. Conversely, reacting acetone over ZnO (20% conversion) produces mesityl oxide and mesitylene in yields of 11 and 1.0%, respectively; however, ZrO_2 generates 15% mesityl oxide and 9% mesitylene yields at 48% conversion at the same reaction temperature and space velocity. Consequently, negligible isobutene yields are observed from the single oxide catalysts under the reaction conditions investigated.

In contrast to the results obtained with the single oxides, a 2:8 physical mixture of ZnO and ZrO_2 generates isobutene from both acetic acid (6.5% yield; 100% conversion) and acetone (10% yield; 80% conversion). The mixture appears to promote the aldol condensation and cracking reactions, as demonstrated by the increased isobutene yield. We observe mesityl oxide yields (including mesityl oxide converted to isobutene) from acetic acid and acetone of 24 and 48%, respectively. Previous reports have shown that simply mechanically mixing and heating ZnO and ZrO_2 changes the acid–base properties of the oxides at the grain boundaries.[33] Therefore, the active sites responsible for isobutene production may be located solely at the interface between ZnO and ZrO_2. Consequently, the frequency of interactive Zn–Zr pairs of the $Zn_xZr_yO_z$ solid solutions was expected to be greater than the simple physical mixture. The isobutene yield from acetic acid over a $Zn_2Zr_8O_z$ amorphous binary metal oxide is 3-fold higher than that obtained for the physically mixed oxide (Figure S1).

The performance of the $Zn_xZr_yO_z$ series was revaluated at optimized space velocities for acetic acid (6.25 g_{feed} $(g_{cat.}\cdot h)^{-1}$) and acetone (4.75 g_{feed} $(g_{cat.}\cdot h)^{-1}$) at 723 K. Over $Zn_1Zr_9O_z$, a 25% isobutene yield was achieved and increasing the Zn content to $Zn_2Zr_8O_z$, further increased the isobutene yield to 48% (Figure 3a). The use of catalysts featuring Zn/Zr ratios higher than 2:8 resulted in decreased yields and in the appearance ZnO reflections in the PXRD diffractograms. Importantly, the activity of $Zn_2Zr_8O_z$ was extremely stable in the presence of the acetic acid feed (See Figure S1a). At lower space velocities, the high yield was maintained for 4 h without appreciable loss of selectivity. A full conversion of the acetic acid was observed in all experiments due to the high ketonization activity for all mixed oxide catalysts. Using acetone as a feed resulted in 50% isobutene yield for all $Zn_xZr_yO_z$ catalysts (ca. 80% conversion and 90% mass balance; Figure 3b).

In comparison to ZrO_2, Tanabe et al. reported that the $Zn_1Zr_1O_z$ oxide possesses lower acidity.[32,34] Even at low Zn to Zr (1:10) ratios, the concentration of Lewis and Brønsted acid sites decreased as suggested by DRIFT spectra of pyridine on the binary oxide.[22] In agreement with these reports, the $Zn_xZr_yO_z$ catalysts possessed fewer acid sites and more basic sites relative to ZrO_2 (see Table S1). Such weak acid–base pairs are capable of catalyzing both ketonization and aldol condensation reactions.[35] At low temperatures and space velocities, ZrO_2 selectively produces mesitylene from acetone, whereas $Zn_2Zr_8O_z$ generates mesityl oxide.[36,37] Mesitylene is the aldol product of mesityl oxide and acetone. Reducing or eliminating certain acid/base sites may be responsible for this shift in selectivity. Additionally, the stability of surface adsorbates is proportional to acid–base strength, and adsorbate-binding strength affects the rates and inhibition (competitive adsorption of ketonization products) of the ketonization reaction.[38,39] Metal ratios must be balanced to efficiently convert acetic acid directly to isobutene. Without competing adsorbates (CO_2 and acetic acid), any ratio of Zn to Zr (up to 1:1) is capable of efficiently converting acetone to isobutene (see Figure 3). The acid–base strength of $Zn_xZr_yO_z$ increases ketonization rates while enabling the cleavage of mesityl oxide.

We hypothesized that the weak Brønsted acid sites on $Zn_xZr_yO_z$ catalyzes the cleavage of mesityl oxide. McAllister et al. reported that mesityl oxide could be cleaved to isobutene and acetic acid over phosphoric acid on silica.[40] To confirm this hypothesis, various possible intermediates were theoretically examined to estimate their stability, as well as their activation upon protonation at different positions (see Table S2). The proton affinity (PA) was calculated as follows: PA = H(mesityl oxide-H^+) − [H(mesityl oxide) + H(H^+)]; this equation was used to determine the stability of protonated mesityl oxide. The protonation at the O of mesityl oxide shows the highest stability of the intermediates (i.e., PA_{MO_O} = −253 kcal·mol^{-1}),

dx.doi.org/10.1021/cs501018k | ACS Catal. 2014, 4, 4196–4200

and at the same time, the C1−C2 bond is strengthened (i.e., the bond length decreased from 1.48 to 1.40 Å). As a result, the C1−C2 bond is less likely to be cleaved due to the presence of a conjugated system among O, C1, C2, and C3 (see MO_O species in Table S2). On the other hand, the protonation of the mesityl oxide carbons results in less stable intermediates than those obtained from the protonation of the mesityl oxide oxygen. The energetic profiles calculated with density functional theory (DFT) indicate that the protonation at C2 (i.e., PA_{MO_C2} = −195 kcal·mol^{-1}) is more favorable than the protonation at the other carbons (i.e., PA_{MO_C1} = −172 kcal·mol^{-1}, and PA_{MO_C3} = −177 kcal·mol^{-1}). In addition, the C2-protonation appears to lead to the stabilization of the partial positive charge at the adjacent tertiary carbon (i.e., C3) and to the elongation of the C1−C2 bond (i.e., the bond length increased significantly from 1.48 to 1.65 Å). Taken together, these calculations suggest a favorable β-scission mechanism to form the corresponding isobutene product (see Scheme S1).

The reaction pathway shown in Scheme 1 was verified by reacting either 1-^{13}C acetic acid, 2-^{13}C acetic acid, 2-^{13}C acetone, or 1,3-^{13}C acetone over $Zn_2Zr_8O_x$ and tracking mass distributions with gas chromatography−mass spectrometry (GC-MS). The distribution of ^{13}C isotopes within product molecules is a function of the position of the ^{13}C label within the carbon backbone of the starting reagent (see Scheme 2).

Scheme 2. ^{13}C-Labelled Reaction Study[a]

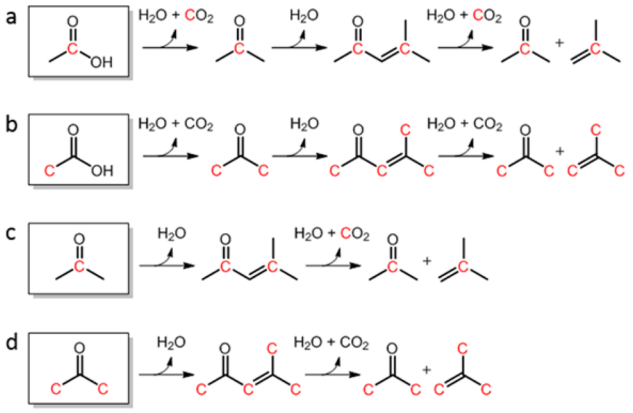

[a]Reactions of (a) 1-^{13}C acetic acid, (b) 2-^{13}C acetic acid, (c) 2-^{13}C acetone and (d) 1,3-^{13}C acetone over $Zn_2Zr_8O_z$ catalyst at 723 K.

The ketonization of 1-^{13}C acetic acid will produce $^{13}CO_2$ and 2-^{13}C acetone while 2-^{13}C acetic acid will yield 1,3-^{13}C acetone. The subsequent homocondensation of 2-^{13}C acetone and 1,3-^{13}C acetone then would generate 2,4-^{13}C mesityl oxide and 1,3,5,5′-^{13}C mesityl oxide, respectively. The cleavage of 2,4-^{13}C mesityl oxide will produce 2-^{13}C isobutene, 2-^{13}C acetone, and $^{13}CO_2$. Reaction of 1,3,5,5′-^{13}C mesityl oxide would generate 1,3,3′-^{13}C isobutene and 1,3-^{13}C acetone. As predicted, starting from either 1-^{13}C acetic acid or 2-^{13}C acetone results in the production of 2-^{13}C isobutene and $^{13}CO_2$ (Scheme 2a,c). However, the reaction of 2-^{13}C acetic acid or 1,3-^{13}C acetone yields 1,3,3′-^{13}C isobutene and unlabeled CO_2 (Scheme 2b,d).

CONCLUSIONS

With unprecedented efficiency, $Zn_xZr_yO_z$ catalyzes a three-step cascade reaction to convert acetic acid directly to isobutene. A 50% isobutene yield was obtained with an optimized $Zn_2Zr_8O_z$ binary amorphous metal oxide. Characterization data relate the weak acid−base pairs to the ketonization and aldol condensation activity, whereas Brønsted acid sites are related to the hydrolysis activity of mesityl oxide to isobutene. However, given the complexity of heterometallic oxides, further research is needed to achieve precise tuning of acid−base pairs at the molecular level. Unlike previously reported Zn−Zr oxides, our materials do not show long-range order representative of independent crystalline domains and thus suggest a very close interaction between Zn and Zr. This inexpensive, robust, and highly active catalyst shows great potential to neutralize and upgrade carboxylic acids for bio-oil upgrading. Current aims in our group focus on upgrading mixed feeds of carboxylic acids commonly found in bio-oil, as well as performing thorough analyses of surface−substrate interactions.

ASSOCIATED CONTENT

Supporting Information

Experimental details; tables including physicochemical properties of various metal oxides, the calculated proton affinities (PA), molecular geometries, and Mulliken charges of mesityl oxide; a figure presenting the conversion of acetic acid over various metal oxides at a WHSV of 25 g_{feed} $(g_{cat.}\cdot h)^{-1}$. This material is available free of charge via the Internet at http://pubs.acs.org.

AUTHOR INFORMATION

Corresponding Author

*E-mail: yroman@mit.edu.

Author Contributions

‡A.J.C. and H.D. contributed equally.

Notes

The authors declare no competing financial interest.

ACKNOWLEDGMENTS

This work was funded by the Cooperative Agreement between the Masdar Institute of Science and Technology (Masdar Institute), Abu Dhabi, UAE, and the Massachusetts Institute of Technology (MIT) (Reference No. 02/MI/MI/CP/11/07633/GEN/G/00).

REFERENCES

(1) Prasomsri, T.; Shetty, M.; Murugappan, K.; Roman-Leshkov, Y. *Energy Environ. Sci.* **2014**, *7*, 2660−2669.
(2) Resasco, D. E.; Crossley, S. P. *Catal. Today* **2014**, DOI: 10.1016/j.cattod.2014.06.037.
(3) Diebold, J. P.; Czernik, S. *Energy Fuels* **1997**, *11*, 1081−1091.
(4) Diebold, J. P. *A Review of the Chemical and Physical Mechanisms of the Storage Stability of Fast Pyrolysis Bio-Oils*; Report No. NREL/ SR-570−27613. National Renewable Energy Laboratory: Washington, DC, 2000.
(5) Oasmaa, A.; Kuoppala, E. *Energy Fuels* **2003**, *17*, 1075−1084.
(6) Oasmaa, A.; Czernik, S. *Energy Fuels* **1999**, *13*, 914−921.
(7) Gliński, M.; Kijeński, J.; Jakubowski, A. *Appl. Catal., A* **1995**, *128*, 209−217.
(8) Pham, T. N.; Shi, D.; Resasco, D. E. *Top. Catal.* **2014**, *57*, 706−714.
(9) Pacchioni, G. *ACS Catal.* **2014**, *4*, 2874−2888.
(10) Deng, L.; Fu, Y.; Guo, Q.-X. *Energy Fuels* **2008**, *23*, 564−568.
(11) Snell, R. W.; Shanks, B. H. *Appl. Catal., A* **2013**, *451*, 86−93.
(12) Snell, R. W.; Shanks, B. H. *ACS Catal.* **2014**, *4*, 512−518.
(13) Prasomsri, T.; Nimmanwudipong, T.; Roman-Leshkov, Y. *Energy Environ. Sci.* **2013**, *6*, 1732−1738.
(14) Wright, M. M.; Román-Leshkov, Y.; Green, W. H. *Biofuel. Bioprod. Bior.* **2012**, *6*, 503−520.

(15) Hutchings, G.; Johnston, P.; Lee, D.; Williams, C. *Catal. Lett.* **1993**, *21*, 49−53.
(16) Dolejšek, Z.; Nováková, J.; Bosáček, V.; Kubelková, L. *Zeolites* **1991**, *11*, 244−247.
(17) Chang, C. D.; Silvestri, A. J. *J. Catal.* **1977**, *47*, 249−259.
(18) Tago, T.; Konno, H.; Ikeda, S.; Yamazaki, S.; Ninomiya, W.; Nakasaka, Y.; Masuda, T. *Catal. Today* **2011**, *164*, 158−162.
(19) Collignon, F.; Mariani, M.; Moreno, S.; Remy, M.; Poncelet, G. *J. Catal.* **1997**, *166*, 53−66.
(20) Mascal, M. *Biofuel. Bioprod. Bior.* **2012**, *6*, 483−493.
(21) Obenaus, F.; Droste, W.; Neumeister, J. Butenes. *Ullmann's Encyclopedia of Industrial Chemistry*; Wiley-VCH Verlag GmbH & Co. KGaA: Weinheim, 2000; Vol. *6*, pp 445−455.
(22) Sun, J.; Zhu, K.; Gao, F.; Wang, C.; Liu, J.; Peden, C. H. F.; Wang, Y. *J. Am. Chem. Soc.* **2011**, *133*, 11096−11099.
(23) Renz, M. *Eur. J. Org. Chem.* **2005**, 979−988.
(24) Pham, T. N.; Sooknoi, T.; Crossley, S. P.; Resasco, D. E. *ACS Catal.* **2013**, *3*, 2456−2473.
(25) 3 Acid and Base Centers: Structure and Acid-Base Property. In *Stud. Surf. Sci. Catal.*; Kozo Tanabe, M. M. Y. O., Hideshi, H., Eds.; Elsevier: The Netherlands, 1989; Vol. *51*, p 27−213.
(26) McFarland, E. W.; Metiu, H. *Chem. Rev.* **2013**, *113*, 4391−4427.
(27) Yakerson, V. I.; Lafer, L. I.; Klyachko-Gurvich, A. L.; Rubinshtein, A. M. *Bull. Acad. Sci. USSR, Div. Chem. Sci.* **1966**, *15*, 65−69.
(28) Gaertner, C. A.; Serrano-Ruiz, J. C.; Braden, D. J.; Dumesic, J. A. *Ind. Eng. Chem. Res.* **2010**, *49*, 6027−6033.
(29) Teterycz, H.; Klimkiewicz, R.; Laniecki, M. *Appl. Catal., A* **2003**, *249*, 313−326.
(30) Gangadharan, A.; Shen, M.; Sooknoi, T.; Resasco, D. E.; Mallinson, R. G. *Appl. Catal., A* **2010**, *385*, 80−91.
(31) Jackson, E. Process for preparing ketones. U.S. Patent US3155730A, November, 3, 1964.
(32) Shibata, K.; Kiyoura, T.; Kitagawa, J.; Sumiyoshi, T.; Tanabe, K. *Bull. Chem. Soc. Jpn.* **1973**, *46*, 2985−2988.
(33) Zhang, W.; Wang, H.; Liao, Y.; Yin, Y. *Catal. Lett.* **1993**, *20*, 243−250.
(34) Tanabe, K.; Sumiyoshi, T.; Shibata, K.; Kiyoura, T.; Kitagawa, J. *Bull. Chem. Soc. Jpn.* **1974**, *47*, 1064−1066.
(35) Climent, M. J.; Corma, A.; Fornés, V.; Guil-Lopez, R.; Iborra, S. *Adv. Synth. Catal.* **2002**, *344*, 1090−1096.
(36) Lippert, S.; Baumann, W.; Thomke, K. *J. Mol. Catal.* **1991**, *69*, 199−214.
(37) Edward, B. E.; Walter, J. P. Preparation of Ketones. U.S. Patent US3153068, October 3, 1964.
(38) Zaki, M. I.; Hasan, M. A.; Pasupulety, L. *Langmuir* **2001**, *17*, 768−774.
(39) Gaertner, C. A.; Serrano-Ruiz, J. C.; Braden, D. J.; Dumesic, J. A. *J. Catal.* **2009**, *266*, 71−78.
(40) McAllister, S. H.; Bailey, W. A.; Bouton, C. M. *J. Am. Chem. Soc.* **1940**, *62*, 3210−3215.